

Enabling Efficient Transaction Processing on CXL-Based Memory Sharing

Zhao Wang
Peking University
Beijing, China
wangzhao21@pku.edu.cn

Yiqi Chen
Peking University
Beijing, China
yiqi.chen

Cong Li
Peking University
Beijing, China
leesou@pku.edu.cn

Dimin Niu
DAMO Academy, Alibaba Group
Hangzhou, China
dimin.niu@alibaba-inc.com

Tianchan Guan
DAMO Academy, Alibaba Group
Hangzhou, China
tianchan.gtc@alibaba-inc.com

Zhaoyang Du
DAMO Academy, Alibaba Group
Hangzhou, China
zhaoyang.dcy@alibaba-inc.com

Xingda Wei
Shanghai Jiao Tong University
Shanghai, China
wxdwfc@sjtu.edu.cn

Guangyu Sun
Peking University
Beijing, China
GSun@pku.edu.cn

Abstract

Transaction processing systems are the crux for modern data-center applications, yet current multi-node systems are slow due to network overheads. This paper advocates for Compute Express Link (CXL) as a network alternative, which enables low-latency and cache-coherent shared memory accesses. However, directly adopting standard CXL primitives leads to performance degradation due to the high cost of maintaining cross-node cache coherence. To address the CXL challenges, this paper introduces CtXNL, a software-hardware co-designed system that implements a novel hybrid coherence primitive tailored to the loosely coherent nature of transactional data. The core innovation of CtXNL is empowering transaction system developers with the ability to selectively achieve data coherence. Our evaluations on OLTP workloads demonstrate that CtXNL enhances performance, outperforming current network-based systems and achieves with up to 2.08x greater throughput than vanilla CXL memory sharing architectures across universal transaction processing policies.

1 Introduction

Transactions provide high availability and strict serializability, simplifying programming and reasoning about concurrency issues. However, scaling single-node transaction systems [75, 77, 86] beyond a node is challenging due to their reliance on shared-memory architectures. When datasets exceed a single node’s memory capacity, a common solution is to employ a distributed transaction system that partitions the data into multiple shards and distributes them across different nodes. This approach utilizes networking techniques, such as RDMA [18, 19, 35, 80], to fetch remote data and synchronize transactions across nodes. However, distributed transactions are notorious for their poor performance, often

attributed to network stack overheads [18, 19, 35, 36, 56, 80]. Despite numerous optimizations in software [35, 36, 56, 80] and hardware [3, 18, 30, 39, 45, 64, 87] aimed at mitigating these issues, they have not fully overcome the inherent performance disadvantages of networking techniques.

The introduction of Compute Express Link (CXL) technologies [16, 67, 68], particularly the CXL 3.0 specification, provides a promising solution for achieving both scalability and efficiency in transaction systems. This technology defines a Global Fabric Attached Memory (G-FAM) node, which allows compute nodes to access G-FAM with memory semantics, and to cache G-FAM data within their processor cache hierarchies. The CXL back-invalidation (BI) scheme maintains cross-node coherence by monitoring and invalidating outdated caches at the CXL fabric using a MESI-like protocol. With the optimized datapath, CXL achieves ultra-low link latency and sub-microsecond G-FAM access latencies [22, 33, 43, 53, 72, 91]. Despite the potential, it remains unknown whether the coherence link of CXL suits transaction processing.

We demonstrate that the vanilla adoption of CXL-based memory sharing in transaction processing systems achieves performance far worse than expected, primarily due to two reasons. First, CXL incurs significant overheads due to "remote cache signal" process which is necessary for coherence maintenance. Here, data loads or stores on G-FAM may notify other nodes’ caches to either invalidate or update their cachelines. This process involves multiple cross-node communication roundtrips over the CXL fabric, with latencies exceeding 800ns in our FPGA prototypes, rendering coherent access 1.85x slower than direct G-FAM DRAM access. Second, to maintain coherence, CXL requires the implementation of an inclusive Snoop Filter (SF) on the G-FAM fabric to monitor the states of cachelines at each node. The SF

presents significant scalability challenges, as its centralized design limits the capacity for memory sharing and the number of compute nodes.

Insights. Our key insight is that the strict coherence model of CXL is overkill for a large fraction of memory accesses in transaction processing systems. In these systems, memory accesses can be classified into record accesses and metadata accesses, based on the type of data they engage. While metadata accesses require strict coherence to ensure synchronization correctness, record accesses typically adhere to well-established transactional consistency models [24, 26, 44], where a record’s store operations are finalized only at the point of transaction commitment. This setup allows for a degree of temporary incoherence among transactions that are still in progress, and transactions that are eventually aborted do not require maintained coherence. However, hardware cannot distinguish between these types without application-provided information. Previous research in concurrency control algorithms, such as SILO [75], supports our observations. Nonetheless, without modifications to underlying hardware mechanisms, these approaches fail to resolve the SF scalability issues. Other works on transactional memory [54, 61, 69, 78] share similar concepts with our findings but are limited to a single socket and are not practical as they necessitate significant changes to processor architectures.

CtXNL-Primitive Innovations. To leverage this insight, we propose a *hybrid* primitive architecture that maintains CXL’s strict coherence for metadata while decoupling coherence maintenance from the memory access process for record accesses. The CtXNL primitive transfers the decision of whether and when to achieve cache coherence from hardware to software, yet still utilizes CXL’s native hardware datapath for coherence operations. By strategically invoking the coherence API, specifically at the point of transaction commitment, transaction system developers can significantly reduce unnecessary cross-node cache coherence overheads. Additionally, software developers can further mitigate cache coherence latencies using techniques such as batching and co-routines, akin to traditional network-based systems.

Architectural Supports. We present holistic architectural support for our CtXNL primitive, designed with the following goals: **G#1:** The architectural design should neither change host processor architectures nor CXL specifications. **G#2:** The architectural design should ensure compatibility with various transaction processing systems’ policies. **G#3:** It is also important to limit implementation overheads to ensure the efficiency of the CtXNL primitive.

To meet these goals, we contribute a hardware-software co-design with three modules: First, we introduce an CtXNL hardware agent (CTHW) at the G-FAM side. The CTHW modifies the semantics of host processors’ loads and stores by remapping them to a node-private address space, and exposing cache synchronization with explicit side-path

API calls. Second, on the host software side, we design a lightweight CtXNL user-level library (CTLib) that allows applications to select primitives for every G-FAM allocation according to application-specific requirements. Third, we propose a user-level runtime thread (CTRt) to monitor CTHW states and reconfigure it according to the use case to maintain efficiency.

Contributions. In summary, this work makes the following contributions:

- We discuss the network-induced performance degradation in traditional distributed transaction processing systems and illustrate how CXL-based memory sharing offers a viable solution (Sec. 2).
- We critically examine the limitations inherent in standard CXL primitives for memory sharing. Through quantitative analysis, we demonstrate that the performance is far below expectations, due to two key performance issues (Sec. 3).
- We introduce a comprehensive solution with a software and hardware co-design approach. We detail a suite of custom primitives (Sec. 4), and describe the systematic and architectural supports of CtXNL (Sec. 5). To the best of our knowledge, this is the first work studying CXL-based memory sharing on transaction processing systems.
- Based on the CtXNL architecture, we implement an exemplary key-value store with a broad exploration of design choices in transaction systems, based on the popular framework DBx1000 [86]. In evaluations using typical OLTP benchmarks, CtXNL reduces over 95% of cross-node coherence traffic and achieves up to 2.08x throughput improvements.

2 Backgrounds

2.1 Network-Based Transaction Processing

Transaction processing is a fundamental component of modern datacenter applications, providing a high-level abstraction that simulates a single host executing a transaction at a time without failure [18, 19]. Current datasets exceed the memory capacity of a single node and are typically partitioned and distributed across multiple memory nodes. This setup necessitates cross-node networking communication for accessing remote records, which can involve great cost. Despite current systems [18, 35, 36, 39, 45, 56, 64, 87] employing various optimization techniques like co-routines and request batching to mitigate network overheads, their performance still greatly degrades if the workload involves remote data accesses. We evaluate the state-of-the-art system DrTM-H under an RDMA cluster with 8 CloudLab’s x170 nodes [20]. As the ratio of remote data access increases from 0% to 100%, its throughput degrades by over 53.3%.

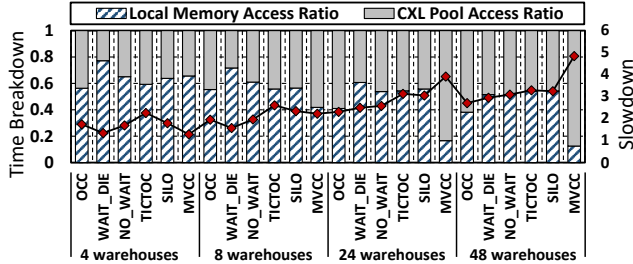


Figure 1. Relative slowdown than *oracle*.

We summarize two primary reasons for this degradation: First, **network stacks’ overhead**. Typical networking fabrics maintain a complex protocol stack to serve a wide range of hosts with robustness against packet loss, yet these stacks incur significant time costs. For example, reading 64 bytes via RDMA can consume over 78% of total latency in copying payloads between buffers within the network stack [22]. Second, **lack of cache coherence support**. Unlike single-node shared memory programming, networking primitives adopt a message-passing model that does not guarantee cross-node coherence at the primitive level. Consequently, it’s common for distributed systems to avoid caching remote data [3, 18, 30, 39, 45, 64, 87] to eliminate software overheads associated with managing coherence. Thus, these systems fail to exploit data locality in applications and involve network communication for every remote data access [35, 79].

2.2 Compute Express Link Basics

Compute Express Link (CXL) is an open industry interconnect standard based on PCIe 5.0 physical links, contributed by a variety of vendors from firmware [2, 40], operating systems [53], and datacenter providers [43, 53]. The recent advancements in the CXL protocol (specification 3.0) introduce a hardware memory sharing programming paradigm [16, 67, 68], which allows external memory, i.e., Global Fabric Attached Memory (G-FAM), to be disaggregated from processing nodes. Multiple compute nodes can share G-FAM by accessing it with standard memory semantics.

The CXL’s memory accessing sub-protocol, `CXL.mem`, enables the read/write memory access primitive at a 64-byte cacheline granularity. Loads and stores via `CXL.mem` are managed with the well-optimized hardware datapath in processors [27, 55], enabling the access latency of G-FAM to achieve sub-microseconds, significantly lower than network-based approaches by an order of magnitude [9, 59, 66, 79]. Another key improvement of CXL is hardware-enabled cache coherence. CXL 3.0 introduces a back-invalidation channel (`CXL.BI`) that allows endpoint devices to invalidate host CPU’s caches. The `CXL.BI` enables the endpoint to retrieve host’s un-flushed dirty cachelines or invalidate stale cachelines using a MESI-style protocol.

2.3 CXL-Based Transaction Processing Systems

One promising CXL-based approach for transaction processing rebuilds the remote procedure call (RPC) layer with a more efficient CXL implementation. This method adapts to the traditional networks’ partitioned architecture, where each node exclusively owns a partition of Global Fabric Attached Memory (G-FAM) and uses RPCs to access partitions from other nodes. Hence, it enables existing network-based systems [11, 15, 49, 73, 76] to migrate to CXL with almost zero code modifications. However, despite being carefully optimized, current SOTA CXL RPCs [50, 88] still suffer from performance overheads due to inherent software control overheads and cache flushing instructions. For example, the HydraRPC [50] exhibits the averaged latency 3.22x longer than directly accessing G-FAM’s DRAM, and consumes considerable CPU cycles on polling the RPC queue. Moreover, partitioned systems work great only if the workload is also perfectly partitionable. As the number of transaction-touched partitions increases, their performance degrade quickly [17, 75].

Another approach involves building a shared memory system leveraging CXL’s cache-coherent memory semantics. This approach employs single-node systems [75, 77, 86] that place shared data structures, including indexes, locks, and tuples, on the G-FAM, allowing worker nodes to run transactions in a multi-threaded manner. The `CXL.BI` ensures hardware-level coherence across nodes. Compared to partitioned systems, this organization better aligns with CXL’s capabilities for cache coherence and exploits data locality, especially beneficial for indexes [51, 79] and locking mechanisms. In this paper, we stick to this shared memory system where each transaction can access the entire dataset. Our evaluations in Section 6 shows that the `CTXNL`-optimized shared memory system outperforms the CXL-RPC partitioned system at most 7.3x on poorly partitioned workloads.

3 Motivations

3.1 Scaling Transactions with Coherent CXL

To investigate how current transaction systems perform under the CXL’s shared memory, we deploy the popular transaction processing framework DBx1000 [86] on the G-FAM. We defer the evaluation details to Section 6.2. Figure 1 illustrates the performance of six commonly adopted concurrency control algorithms on the TPC-C benchmark [74]. The numbers are normalized to an *oracle* architecture that operates on local DRAM and consolidates all worker threads within a single socket. We group the time components based on the memory modules accessed by the transactions. It is evident that CXL memory sharing slows down all algorithms by 2.51x on average, with 46.89% of the time spent on accessing G-FAM. Algorithms that maintain multiple tuple versions, such as `MVCC`, experience the most significant performance loss, since they require more CXL memory accesses to create

new tuple versions and reclaim the stale ones than those maintaining only a single tuple version.

3.2 CXL’s Coherence Cost

CXL’s memory sharing, along with most caching architectures [9, 52, 59, 62, 89, 90], adopts the *strictly coherent* cache model [6, 7] to simplify software development. The basic design principle of this model is to ensure a single, global order for all memory locations. A memory store in the strictly coherent model is only completed once all peer nodes have observed it. This order is also known as the single-writer-multiple-reader invariant [55], which allows only a single node to execute a write primitive on a location or multiple nodes to execute read primitives at the same time. In subsequent discussions, we refer to the primitives that adhere to this coherence model as “CXL-vanilla.”

Maintaining such a coherence model requires complex hardware logic to send coherence requests and track the lists of sharing nodes. In CXL, this is achieved through an MESI-like ownership-based (write-back) coherence and directory-based communication [5, 12, 27, 55]. Write-back coherence means that a cache write is not immediately reflected in the DRAM but instead marks the cacheline as dirty. Consequently, a cache read miss retrieves the content from a remote dirty cache rather than directly from the memory. Directory-based architecture implies that the hardware maintains a directory to track which caches hold each cacheline and their states. A cache controller intending to issue a coherence request first sends it to the directory to determine which node is holding the peer caches. Such a directory is implemented as a Snooper Filter (SF) in CXL specifications.

3.2.1 Remote Cache Signaling Cost. In order to maintain the strict coherence model, CXL-vanilla introduces a remote cache signaling process to invalidate a remote cacheline for exclusive ownership requirements or to retrieve the contents for a read miss. Figure 2 (a) illustrates an example where a cache read miss on node-2 retrieves a modified cacheline from node-1 via the CXL fabric. This process involves two CXL request-response roundtrips between the host and the G-FAM node: one for node-2’s read request to the G-FAM, and another for the read request from G-FAM to node-1. Each CXL roundtrip is designed to take about 75ns with an ideal ASIC implementation [22, 43, 53, 68], and the currently available FPGA-based platform exhibits an average latency of approximately 400ns [28, 50, 72]. We develop a real-world prototype system utilizing these off-the-shelf hardware. As illustrated in Table 1, the remote cache signaling roundtrip takes approximately 850ns, which is 3.4 times greater than the latency of an ideal ASIC implementation. This gap is primarily due to the low operational frequency of FPGA’s CXL IP and the intrinsic overhead associated with this FPGA’s chiplet architecture. We will detail this prototype in Section 6.2.

Table 1. Roundtrip Latency Comparison

	Socket	NUMA	CXL (Ideal)	CXL (Proto)
Core-to-Mem	92ns	145ns	170ns	456ns
Core-to-Core	49ns	133ns	246ns	847ns
C2C/C2M	0.53x	0.91x	1.44x	1.85x

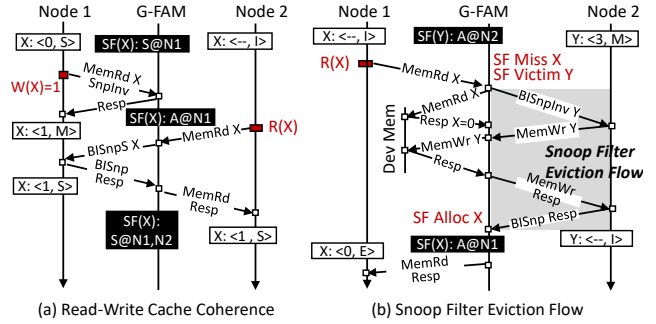


Figure 2. (a) Remote cache signaling to node-1 from a node-2’s read. (b) SF eviction process incurred by node-1’s read.

In addition to the significant link latency, CXL introduces a unique coherence bottleneck when a read miss is served by the remote dirty cache. Previous works [43, 63] have adopted the non-uniform memory access (NUMA) architecture as a mimic of CXL memory. However, such a mimic is not adequate in the memory sharing since CXL exhibits relatively larger latency in remote cache signal time compared with conventional NUMA interconnects, such as the Quick-Path Interconnect (QPI) [32]. As shown in Table 1, in most commercial NUMA architectures [46, 85], reading a remote cacheline is not overly costly since the NUMA remote signal time is similar to accessing local memory. However, in CXL, the remote cache signal takes 44% to 85% more time than the latter, primarily because CXL requires two link roundtrips to inform other nodes, whereas NUMA only takes one. As the cluster size increases, the latency gap tends to expand, primarily due to the potential overhead introduced by retimers and CXL switches [43] associated with the CXL link. An increase in roundtrip latency could exacerbate the overhead of remote cache signaling process.

Take-away#1: Remote cache signaling makes considerable performance overheads on G-FAM accesses.

3.2.2 Snooper Filter Scalability Issues. To enable cross-host cache coherence, the CXL endpoint should maintain a snooper filter (SF) to track the ownership of cachelines associated with the address space of G-FAM [29, 46, 85]. The SF should be inclusive of the G-FAM’s cachelines in all processors’ local caches. This means the SF needs to track which nodes hold the cacheline and in what states, if the cacheline is located in at least one node’s cache. Every unique G-FAM load or store should occupy an SF entry.

Compared with the SF in NUMA architectures, CXL SF faces unique scalability issues due to its centralized design. The CXL SF is located only at the G-FAM node and tracks all hosts’ accesses, whereas NUMA architecture distributes SFs across every socket, with each SF tracking only remote accesses to its own socket. We use the existing NUMA SF design as a mimic since a specific CXL SF design has not yet been proposed. To support a common rack-scale cluster with 16 nodes, the CXL endpoint is expected to maintain a 64K-set 11-way on-chip SF, which is 16x larger than a single NUMA SF in the current Intel Skylake architecture [29, 85]. In the worst case, where all processors’ valid cachelines cache the G-FAM contents, the SF would require 1.8 billion entries and consume 14.4GB of memory. As the number of nodes increases, the CXL SF should expand correspondingly and could easily become a system bottleneck.

Conflicts on the SF lead to an SF eviction flow that back-invalidates other cachelines [16, 68] to make room for SF allocation. Figure 2 (b) illustrates an example: a read on X, which is not currently recorded by the SF, incurs an SF eviction on Y since they map to the same SF slot. The EP must wait for the eviction flow to reach node-2 before responding to node-1’s read request. Such a process involves three CXL roundtrips on the critical path, which take over 400ns more than the remote signaling process.

Take-away#2: The centralized snoop filter causes scalability issues of CXL-vanilla primitives.

3.3 Do transactions require strict coherence ?

We observe that the coherence model adopted by the CXL-vanilla primitives is overkill for most transaction processing systems. We use the key-value store (KVS) as an example. A typical KVS comprises two data fields: the *record field*, which stores the actual data (KVS’s value) managed by the system, and the *metadata field*, which contains the system’s internal data structures to ensure transaction correctness, such as locks, timestamps, indexes, and latches.

Accesses to the *record field* follow a much looser order than what CXL’s strict coherence model provides. Specifically, accesses to the *record field* are all wrapped within transactions that are committed as all or none. These accesses thus adhere to specific transactional consistency models [26], such as strict serializability [24] or snapshot isolation [44]. These consistency models permit reads from two or more transactions to observe temporarily incoherent values. Figure 3 illustrates an example of a strict serializable consistency model, where the read from Txn-4 precedes Txn-2’s write, despite this read occurring after the write in physical time.

Such counter-intuitive ordering is maintained by the concurrency control algorithms in transaction processing systems. Therefore, there is no need for the hardware to maintain the strict cache coherence model, which incurs substantial performance overheads (Take-away #1 and #2). As an

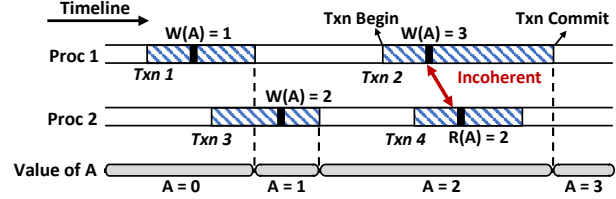


Figure 3. The strict serializable consistency.

alternative, the hardware could simply maintain the partial order required by transactional consistency, allowing data incoherence according to the transaction’s execution status and synchronizing data only at the commitments of transactions [1, 7, 24, 37, 42, 61, 70, 78].

Prior works on single-node concurrency controls, such as SILO [75], align with our findings but their solutions are orthogonal to us. Specifically, SILO aims to avoid unnecessary coherence traffic incurred by *metadata* writes that are required for read-only records’ accesses, but it can not mitigate the remote signal costs associated with *record* accesses themselves, hence it can not address the remote singling cost on records accesses. Moreover, SILO-like concurrency controls only modify the software algorithms, which do not address SF issues without changes to the underlying hardware coherence mechanisms.

Take-away#3: Transaction processing systems allow the record field accesses to be temporal in-coherent.

4 CTXNL Overview

4.1 CTXNL Primitives

To exploit the incoherence opportunity in the record field (Take-away#3), we propose a hybrid primitive design that implements different protocols depending on the field accessed by the primitive. Users can employ the strictly coherent protocol for the *metadata field* to ensure the correctness of atomic operations. For the *record field*, CTXNL advocates for a new, loosely coherent protocol. In the following discussion, we use “CTXNL primitive” to indicate the *record field* primitives for simplicity. The CTXNL primitive decouples costly cross-node coherence operations in CXL from normal memory accesses. It comprises four fundamental memory operations: Local-Load (L-Ld), Local-Store (L-St), Global Synchronization (GSync), and Withdraw (Wd).

L-Ld and L-St retrieve and put data from/to the shared memory, and their effects are limited to the requesting node, making no coherence demands. We utilize litmus tests [89] to compare L-Ld and L-St with standard CXL Loads (Ld) and Stores (St). As depicted in Figure 4, P1 forwards the value from I1 to I2 and I3 locally without making I1 visible to P2 at N2, allowing r2 and r4 to both be 0 simultaneously. In contrast, with CXL-vanilla primitives, if both I2 and I3

Proc. P1 @N1	Proc. P2 @N2
I_1 : St/L-St α 1	I_4 : St/L-St β 1
I_2 : r1 = Ld/L-Ld α	I_5 : r3 = Ld/L-Ld β
I_3 : r2=Ld/L-Ld(β +r1-1)	I_6 : r4=Ld/L-Ld(α +r3-1)
CXL-vanilla forbids but CtxNL guarantees: r1 = 1, r2 = 0, r3 = 1, r4 = 0	

Proc. P1 @N1	Proc. P2 @N2
I_1 : St/L-St α 1	I_5 : St/L-St β 1
I_2 : r1 = Ld/L-Ld α	I_6 : r3 = Ld/L-Ld β
I_3 : GSync α	I_7 : GSync β
I_4 : r2=Ld/L-Ld(β +r1-1)	I_8 : r4=Ld/L-Ld(α +r3-1)
CtxNL forbids: r1 = 1, r2 = 0, r3 = 1, r4 = 0	

Proc. P1 @N1	Proc. P2 @N2
I_1 : St/L-St α 1	I_5 : St/L-St β 1
I_2 : r1 = Ld/L-Ld α	I_6 : r3 = Ld/L-Ld β
I_3 : Wd α	I_7 : GSync β
I_4 : r2=Ld/L-Ld(β +r1-1)	I_8 : r4=Ld/L-Ld(α +r3-1)
CtxNL forbids: r3 = 1, r4 = 1	

Figure 4. L-Ld and L-St are node-private

Figure 5. GSync broadcasts stores

Figure 6. Wd withdraws stores.

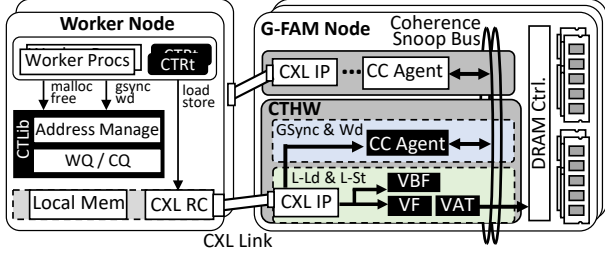


Figure 7. CtxNL overview.

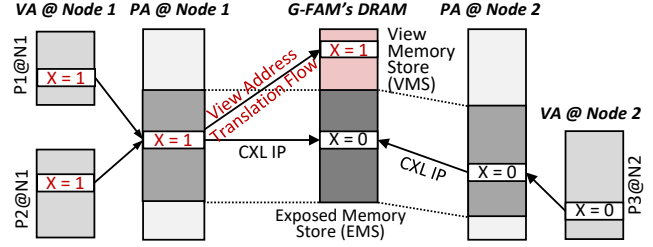


Figure 8. View memory shim.

return the value 1, it implies that stores I1 and I4 must have been globally observed, hence r2 and r4 cannot both be 0.

The GSync broadcasts a node-private value globally, while the Wd withdraws updates made by preceding L-Sts that have not yet been broadcast. The synchronization primitives should be specified for a particular address. As depicted in Figure 5, following the GSync primitives, both P1 and P2 can observe the new value stored by I1 and I5. Consequently, I4 and I8 cannot both be 0, similar to the behavior observed with CXL-vanilla primitives. As illustrated in Figure 6, Wd cancels the value stored by I2 so that it is invisible to I8.

4.2 Design Challenges

Challenge#1: Being Compatible with Processor Cache Design. Implementing L-Ld and L-St requires isolating accesses across nodes. Merely disabling the CXL.BI for shared memory accesses does not suffice to implement L-Ld and L-St due to cache eviction issues. Recall that CXL uses write-back protocols [16, 68], meaning that stores always hit local caches. However, cache eviction can inadvertently leak modified contents from the private cache to the shared memory, allowing subsequent loads from other nodes to observe these modified contents. Worse still, cache eviction is managed by uncore cache agents, which operate transparently to cores.

Challenge#2: Being Compatible with CXL Protocols. The CXL protocol does not differentiate between cacheline flushing and eviction; both are treated as CXL.mem write-back requests. This conflation prevents the use of cacheline flushing as a synchronization point (to implement GSync), which was possible in earlier weakly consistent architectures [4, 5, 89, 90]. Moreover, current x86 architectures do not support the Wd semantic that merely self-invalidates a cacheline without writing it back.

Challenge#3: Being Compatible with Software Policies.

To fully exploit the advantages of the hybrid primitive, our system should allow application processes to choose which primitive to use for each data structure they allocate. Simply partitioning the address space to map to different primitives is too rigid to accommodate the diverse requirements of various use cases.

4.3 Architecture Overviews

CtxNL integrates multiple components to address these challenges. As Figure 7 shows, we employ a hardware agent (CTHW), which implements CtxNL primitives in the G-FAM to address the cache eviction problem for L-Ld and L-St (**Challenge#1 and #2**) and to enable synchronization primitives with a different mechanism (Sec. 5.1, 5.2, and 5.3). Additionally, a user-level library (CxLib) facilitates the selection of memory primitives for individual data structures (**Challenge#3**), enhancing software integration with the hardware capabilities (Sec. 5.4 and 5.5). Moreover, a helper thread (CTRt) adjusts the hardware configuration to maintain system efficiency (Sec. 5.6).

CtxNL adopts a non-transparent interface for memory management calls such as `cxl_alloc` and `cxl_free`, but keeps accessing approaches the same as local memory. System developers can bind the primitive to each allocation with passed arguments and load or store data as they would with local memory. At the point of transaction commits, the developer should invoke the GSync primitive to synchronize record writes globally, and if the transaction aborts, they should call the Wd primitive to withdraw stores.

5 CTXNL Architectural Supports

5.1 View Memory Shim

In the following discussion, we first focus on the architectural support of the loosely coherent model and leave the integration of hybrid models to Sec. 5.5. In this section, we illustrate the core conceptual model of our design, named view shim layer. The view shim layer operates between the node’s physical address space and the G-FAM DRAM address space, aiming to redirect memory accesses from nodes to the appropriate G-FAM DRAM locations according to L-Ld and L-St semantics. We adopt the concept of “view” from relational databases [21, 65, 78]. As Figure 8 shows, each physical address can be mapped to a DRAM location called a view shim, in addition to a regular DRAM location mapped by the CXL IP. At a high level, when a physical address has both an original DRAM mapping and a view shim mapping, the L-Ld and L-Sts are served by the view shim. Only addresses not present in the view shim are accessed from the regular DRAM location. Each node can own at most one view shim for a shared object, but views from different nodes are isolated. In this example, the physical object X is mapped to both the original DRAM address space and a view shim in node-1, while node-2 only has the DRAM mapping. Consequently, the process in node-1 observes X=1, while the process in node-2 observes X=0.

Logically, a view shim is created on a memory store and is merged with the original memory location upon a GSync call, resembling copy-on-write semantics. Physically, the view has two statuses: on-chip and overflowed. The on-chip view resides within the processor’s cache hierarchy as a common dirty cacheline and transitions to the overflowed status once it is evicted from the processor. A view starts in the on-chip status since any store would first load the cacheline to the processor followed by a store hit.

The on-chip view naturally fits the L-Ld and L-St semantics as it is only observed by local loads and stores. However, the G-FAM needs to ensure that overflowed views are not observed by other nodes. To achieve this, we allocate a DRAM space called the view memory store (VMS) to buffer the overflowed views, acting as an evicted cache. We term the DRAM space that stores original shared contents as the exposed memory store (EMS) and maintain the address mapping between EMS and VMS via the node-wise view address translation flow.

5.2 View Address Translation Flow

The view address translation flow controls whether the G-FAM returns a read request with the view in VMS or the original content in EMS, and it allocates space for overflowed views. It does not change the CXL IP but operates behind it. The CXL IP retrieves and translates the physical address to the EMS address [16, 28]. Our flow takes this decoded information as input and outputs the target DRAM address

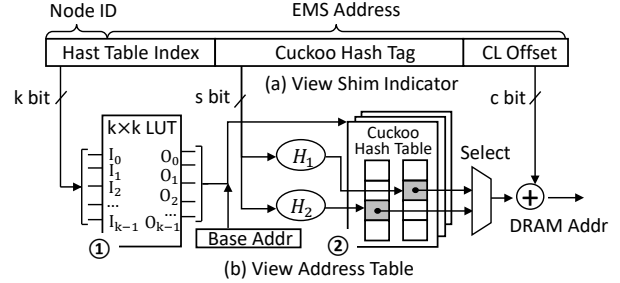


Figure 9. (a) The format of view shim indicator and (b) View address table (VAT) components.

according to the view shim model. We architecturally define three data structures: the view address table (VAT), which manages the mapping from the view shim indicator to the VMS address; the VMS filter (VF), which precedes the VAT to sift its query traffic; and the VMS Back Filter (VBF), which tracks the processor caches.

5.2.1 VAT Details. A VAT entry (VATE) holds the address mapping at cacheline granularity. The VAT resembles OS page tables in functionality, but traditional radix-tree-style page tables are not suitable for our scenario since address translation involves page table walks that potentially traverse all levels of the tree sequentially [23, 71]. To address this, we adopt a flattened cuckoo hash table architecture that bounds the number of view address translations within a limited number of DRAM accesses. As Figure 9 (b) shows, we organize the VAT as a variable list of cuckoo hash tables [57, 71]. The rationale behind choosing cuckoo hashing is to trade the low cost of L-Ld with the insertion overhead of L-St, since an L-Ld typically lies on the critical path, whereas an L-St does not, due to current processors’ out-of-order execution and asynchronous cache eviction [27, 55, 89, 90].

An on-chip lookup table (①) stores the hash table base addresses, and the hash tables are located in the VMS (②). We use the first k bits to calculate the table’s base address and the following s bits to query the cuckoo hash tables. The cuckoo hash table maps one key to two possible hashing locations using different hash functions. An element is stored in only one of these locations at a time but can be relocated between them. An L-Ld operation introduces a cuckoo hash query, which checks both locations and returns success if the element is found in either. If no valid VATE is located, it reverts to the original EMS address. An L-St operation initiates a cuckoo hash insertion, placing an element in one of the two possible entries. If the chosen entry is already occupied, the algorithm displaces the current occupant, attempting to re-insert it at the alternative hashing location. This displacement process continues until it succeeds without eviction or reaches the maximum number of allowed retries.

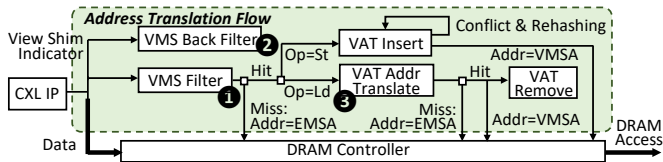


Figure 10. Address translation process for L-Ld and L-St.

There are two potential performance inefficiencies in this VAT design. First, a VAT insertion may require memory allocation for the cacheline content, in addition to inserting the VATE to the hash table. To mitigate this, we pre-allocate buffers for cacheline contents associated with the hash table. Second, cuckoo hash insertion may fail after reaching the maximum number of retries. Upon such a failure, the CTHW blocks all accessing to the hash map, sets the resizing error bit, signals the CTRt to resize VAT and retries the insertion (Sec.5.6). Nonetheless, the occurrence of such an insertion failure is very infrequent in practice, as the CTRt actively oversees VAT occupancy to keep it within a moderate level. A threshold of 0.6 guarantees that an insertion is typically accomplished within 6 retries. We will discuss this at Sec. 6.6.

5.2.2 VF and VBF Details. Despite the VAT optimizing DRAM address translation, it still impacts performance since every memory access must check the VATE in DRAM. However, most VAT queries would miss for two reasons. First, stores are relatively rare in real-world transaction applications [47, 48], so the VMS is typically sparse. Second, most views reside in host processor caches and are seldom written back to the VMS due to widely adopted LRU-based cache eviction policies.

To leverage this feature, we introduce an on-chip VMS Filter (1 in Figure 10, VF for short) to sift out VAT queries. A read on the shared memory would query the VF first, accessing the VAT only if the filter outputs a positive hit. Otherwise, the read falls back to the original EMS address. CTHW also tracks the host processor’s caches to invalidate stale cachelines at synchronization (detailed in Sec. 5.3). Consequently, each CTHW maintains a VMS Back Filter (2, VBF for short) that works in reverse to the VF: a DRAM load inserts into the VBF, and a dirty write-back removes from the VBF. Compared with the original CXL SF, the VBF has three advantages: First, VBF is organized in a distributed way, so that each VBF only tracks the local processor’s cache, avoiding a single VBF becoming the system’s bottleneck. Second, VBF queries and inserts are parallel with VF accesses, thus introducing minimal overhead to the memory access critical path. Third, the VBF exhibits much higher spatial efficiency when implemented with approximate data structures, such as elastic counting bloom filters [82].

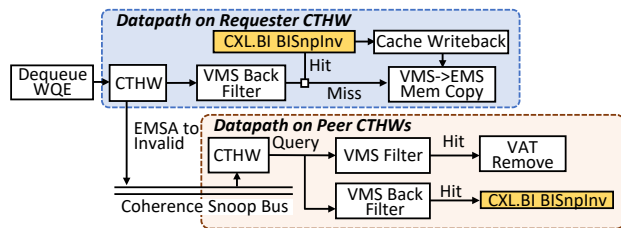


Figure 11. Synchronization datapath for GSync and Wd.

5.3 View Synchronization Flow

5.3.1 Task Offloading Scheme. Different with the view address translation flow that works “on the path” of memory accesses, the GSync and Wd primitives are implemented in task offloading scheme. The endpoint maintains a queue pair for each host: a work queue and a completion queue. The host posts the addresses for GSync and Wd in the work queue element and polls the completion queue to synchronize for completion. The work queue is a circular buffer, while the completion queue is a bit vector where each bit maps to a work queue element. Both queues are located in the shared memory between hosts and devices and are accessed coherently utilizing the CXL . cache sub-protocol. Inspired by the CC-NIC [63], we apply an inline signal scheme to ensure only one coherent read is needed to retrieve the entire work queue element. Instead of signaling work queue changes with an explicit flag, we embed a valid bit into each work queue element. The endpoint polls the header element’s valid bit and reads the payload once it observes that the valid bit is set. To further reduce coherence traffic, we limit the size of completion queue to a cacheline to enable one CXL . cache read to get all pending completion queue elements.

5.3.2 Achieving Coherence Across Nodes. Synchronizing a dirty view involves two phases: invalidating the cachelines on remote nodes and merging the dirty view with the EMS. As Figure 11 shows, we refer to the CTHW executing the GSync as the *requester* and other CTHWs as the *peers*. During remote cache invalidation, the *requester* broadcasts an invalidation message on the coherence snoop bus. Each *peer* checks its own VF and VBF to determine if it holds the corresponding cacheline in either on-chip or overflowed status. If the view resides in the VMS, the *peer* simply invalidates the VAT entry to remove it. If it resides on-chip, the *peer* invalidates the host processor’s cacheline by issuing a standard CXL .BI invalidation request [16, 68]. The CTHW ignores the written-back value since it’s outdated.

The content merging phase encounters two scenarios: the modified cacheline either remains in the host’s cache or has already overflowed to the VMS. The *requester* checks its VF and VBF to determine the status. If the cacheline is on-chip, the *requester* sends a CXL .BI invalidation request to the host to force a cacheline eviction, then writes the evicted data to

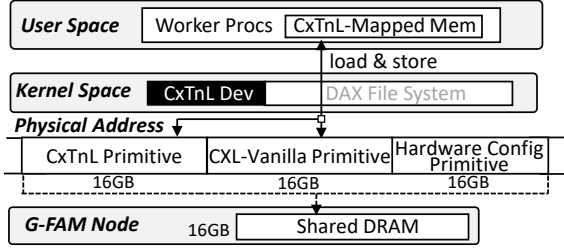


Figure 12. The CTXNL’s memory mapping to OS.

the EMS. Otherwise, the *requester* performs a memory copy from the VMS to the EMS and invalidates the VATE.

5.4 Operating System Integration

Resembling the Persistent Memory Development Toolkit (PMDK) [58], CTXNL adopts the Direct Access (DAX) mechanism to manage the shared memory [22, 33, 88]. We expose the device as a DAX file and allow the application to *mmap* the G-FAM to its virtual address space. We do not adopt previous approaches of exposing the G-FAM as a zero-core virtual NUMA node [43, 53], i.e., a node with memory but no cores, since it is costly to use current NUMA control approaches to precisely specify the memory node at allocation.

In this work, we set all G-FAM pages as “reserved” in the BIOS to prevent OS intervention, such as page swapping. This ensures that RTLlib has full control to allocate the entire G-FAM to a contiguous virtual address segment for applications. The combination of DAX mode and page reservation ensures effective address translation among the virtual address space that CTLlib operates on, the physical address space that the on-chip cache operates on, and the endpoint’s DRAM address space that CTHW operates on, as it maintains a linear address mapping between these spaces.

5.5 Memory-Mapped Primitive Selection

To enable multi-primitive selection, we expand the concept of memory-mapped I/O. As Figure 12 illustrates, the CTXNL driver exposes the G-FAM to a physical address region with three times larger capacity. Each segment maps to a different primitive, including the CXL-vanilla primitive with hardware-managed strict coherence, the CTXNL primitive with decoupled coherence, and a special hardware configuration primitive for internal data structures of CTXNL, such as VAT’s hash tables, VMS contents, and work/complete queues. Applications could specify the CXL-vanilla primitive or the CTXNL primitive via CTLlib’s APIs, while the hardware configuration segment is reserved for CTXNL internal usage so that it is transparent to users. To avoid overlap between the application data and CTXNL data, we adopt a virtual address management strategy where the application address segment grows from the bottom base address upward, while the

hardware configuration segment expands from the top address downward. When two segments overlap, i.e. no unused memory exists, an out-of-memory error occurs.

We allow transaction processing systems to manage application address segments with customized allocators but allocation should be aligned with cacheline to match CXL protocol granularity. Conversely, CTRt are required to manage the hardware configuration segments. CTRt handles memory allocation and reclamation in fixed-sized chunks. Previously freed chunks are stored in a doubly linked list. Allocating a chunk in the hardware configuration segment first searches this list using a first-fit strategy. If no adequate chunks are available, CTRt expands the hardware configuration segment to satisfy this allocation. While advanced memory management strategies such as segregated free lists could enhance performance, delving into these methods is beyond the scope of this paper, thus we defer their exploration to future works.

5.6 VAT Resizing

The VAT resizing mechanism adapts the concept of page swapping daemon of virtual memory subsystems. To be specific, we introduce a helper thread CTRt to monitor the VAT’s occupancy and conducting VAT resizing. At every I milliseconds, the CTRt checks the occupation ratio of each hash table. The ratio is managed by the CTHW at hardware and is exposed through the hardware configuration address space. We introduce VAT expansion in this section, and VAT shrinking works in the reverse manner. If a table t_{old} meets the occupancy threshold r , the runtime initiates a VAT expansion procedure to increase the t_{old} to a table with $k \times$ equivalent capacity. The CTRt increases the number of hash tables to accommodate t_{old} ’s VATES. CTRt creates $k - 1$ additional cuckoo hash tables with the same hash functions. CTRt scans the table base address LUT and moves the t_{old} ’s VATES with the prefix s_i to the new hash table $t_{new_{i \times k}}$. The table bias of the VATE in $t_{new_{i \times k}}$ is the same to the t_{old} thus avoiding the rehashing cost. After migration, CTRt updates the on-chip LUT to point the prefix to newly created hash tables. If the LUT is full that each s_i points to an unique table, CTRt falls back to the rehashing.

To prevent data races between CTRt and worker threads, CTRt temporarily blocks any access to the hash table that is manipulated by the VAT resizing process. This involves negligible impact on overall performance, as VAT resizing occurs infrequently. The reasons are twofold. First, the VAT occupancy capacity is determined by the number of *pending writes* from uncommitted transactions. Given that OLTP transactions are typically read-intensive and short-lived [47, 48], the volume of pending writes is inherently limited in OLTP workloads. Second, the large on-chip caches is the primary location of pending writes, leaving VAT to manage only a minor fraction of the pending write set.

Table 2. System Parameters and Configurations

Host Processors	
Processor	10-core @ 3.2GHz
L1/L1D/L2/L3	32KB,4way / 32KB,8way / 2MB,8way / 1.875MB,16way
Memory System	2x channel, 64GB, DDR4 @2666MHz
CXL Configurations	
Connection	32Gb/s/Lane, 8x Lanes (32GB/s) per node
Memory	DDR4 @2666MHz, 21.3GB/s/channel, 8x channels (170.4GB/s in total)
Snoop Filter	128K entries, 16 way
CxTnL Parameters	
VF/VBF	512B per node,2 hash / 16KB per node,2 hash
VAT	1M entries/hash table, 2-way, 40 bit index, resizing threshold=0.6/0.01, interval=10ms

6 Implementation and Evaluation

6.1 Exemplified Transaction Key-Value Store

We construct a shared record key-value store (KVS) based on the CTXNL architecture. Similar to recent works [34, 35, 39, 45, 56, 64, 80, 81], we adopt a shared-record organization where transactions on any node may manipulate any records of the dataset. Nodes execute in a symmetric model [18, 35, 80, 81], where each node runs both client and server processes. Note that CTXNL is also compatible with other organizations, such as shared-nothing architectures [11, 15, 49, 73, 76] and deterministic scheduling [60, 73]. We adopt the widely used framework DBx1000 [83, 86] as our codebase. The KVS uses either a hash table or a tree to store the key-value items. Taking hash index as an example, each key maps to a bucket, and the bucket is organized as a linked chain. A bucket item contains a pointer to the tuple header, which further points to the value. We bind only the records with CTXNL primitives, while other shared contents, including indexes and headers, remain with CXL-vanilla primitives.

6.2 Setups

Benchmarks. Following previous in-memory transaction processing works [25, 77, 80, 81], we adopt two OLTP tasks: (a) TPC-C [74], the current industry standard for OLTP evaluation. Similar to previous works [25], we adopt two (Payment and NewOrder) out of five transactions in our simulation as a default mixture (DM) since they account for 88% of the TPC-C workload, and also tests NewOrder-only cases (NO). (b) YCSB [13], representative of large-scale cloud services. In this paper, we use a 16GB YCSB database containing a single table with 16 million records. Each tuple has a single primary key and 10 values, each with 20 bytes of randomly generated string data. A transaction accesses 16 records with reads or writes controlled by write ratio w , and follows the Zipfian distribution controlled by the skew factor θ .

Evaluation Methodology. We develop an FPGA-based CXL memory system, incorporating an Intel® Sapphire-Rapids™

Xeon Gold 6430 CPU and an Intel® Agilex™-7 I-Series FPGA configured as a CXL type-2 device (CXL 1.1). This configuration enables both CXL .mem and CXL .cache of the CXL IP [14]. The CXL IP consists of a hardware component, implemented as an independent chiplet known as R-Tile [14], and a soft-encrypted wrapper located within the Programmable Logic (PL) domain, working at 400 MHz. The inter-chiplet communication between the hard and soft components of the CXL IP introduces a significant portion of the overall latency. The FPGA owns dual-channel DDR4-2666 memory, totaling 16GB in capacity. The memory system operates under Linux kernel v6.3.

With this prototype, we evaluate two key performance features that determine the CXL protocol latency: the host-to-device CXL .mem roundtrip latency and the device-to-host CXL .BI roundtrip latency. To evaluate the first phase, we employ the approach used in prior studies [72, 91] that adopts the standard memory latency checker [31] to generate loads and stores from the host CPU to the device memory. To mimic the snoop-filter behaviors as mentioned Figure 2, we implement a direct-map SF at the FPGA PL side, locating at CXL .mem critical path and do updates at each memory accesses. This number is known as C2M latency in Table 1. For the second phase, we utilize CXL .cache to emulate the datapath of CXL .BI since it is not yet available in CXL 1.1 devices. CXL .BI have similar protocol roundtrip constitution with CXL .cache, and it is introduced in 3.0 to avoid the circular channel dependence between CXL .cache and CXL .mem [16, 67, 68]. We construct a test core on the FPGA’s PL side to generate memory access requests. These requests are routed to the CXL IP in host-bias mode via the AXI bus, initiating CXL .cache requests from the device to the host [14, 16, 68]. The test core waits for the accessed data to be returned and records the total latency. To get the pure CXL link latency, we subtract the two aforementioned numbers with the time that PL test core spends on accessing the device memory without intervening CXL IP. We add the two subtraction results to get C2C latency.

Due to the deadlock issue from CXL .cache’s channel dependency [16, 67, 68], we are unable to conduct full system evaluation based on the prototype FPGA. We thus develop a pin-tool simulator based on Sniper [10] with around 2.5K LoC changes. We build a memory node that simulates the CTXNL and CXL-vanilla architecture based on the performance characteristics of the prototype. We change a few lines of DBx1000 to adapt to CTLib. We also assess the ideal ASIC performance in the simulator based on reports from chip vendors and IP providers [2, 22, 53, 84], as detailed in Table 1. For network-based systems, we deploy the distribution version of DBx1000 [25, 86] on 8 r320 nodes in CloudLab [20].

Simulation Setups. Table 2 summarizes the default system configurations. Each node equips with an OoO CPU with the Intel Xeon Gold 6430 architecture (Sapphire Rapids series).

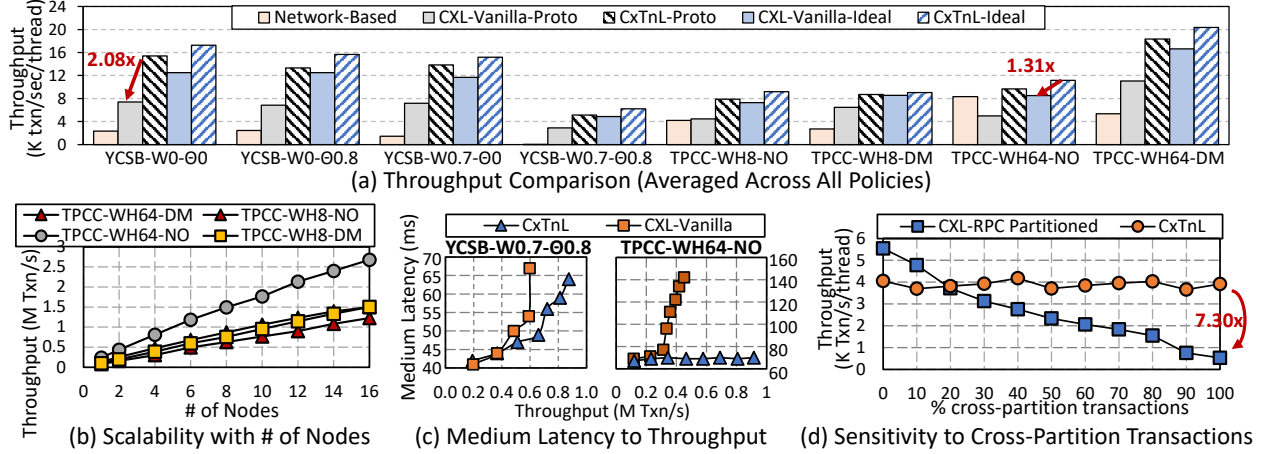


Figure 13. Overall Performance Comparison.

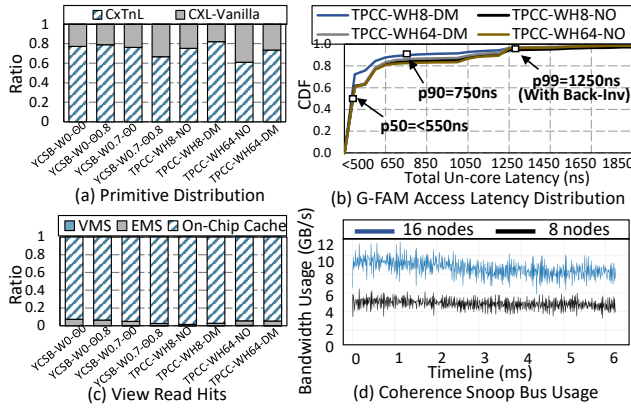


Figure 14. Detailed Analysis of CxTnL.

For CXL architecture, we equip each node with an P2P CXL $\times 8$ connection with EP. The EP manages shared memory in 8 channels with interleaved addresses in cacheline granularity. The EP manages an 16 way on-chip SF with 128K-entries. For CxTnL architecture, each CTHW implements VF and VBF via 512B and 16KB bloom filters with 2 hash functions by default. The view shim indicator takes 56 bits with 4 bit node id and 48 bit EMS address. The most significant 16 bits index the on-chip LUT, the following 40 bits calculates the cuckoo hashes.

6.3 Main Results

Figure 13 (a) presents a performance comparison between our proposed CxTnL and baseline primitives, with throughput averaged across all transaction control policies in the benchmark to neutralize algorithmic effects. The results highlight CxTnL’s consistent performance gains over CXL-vanilla systems, achieving a 1.36x improvement in ideal ASIC setups and 2.08x in prototype setups. Specifically, CxTnL exhibits greater enhancements in the memory-insensitive

YCSB benchmarks (93% on average) compared to the TPCC benchmarks (77% on average), due to TPCC’s higher computation burden. Moreover, CxTnL outstrips traditional networking-based architectures by 6.47x, leveraging the superior performance of the CXL protocol while circumventing the inefficiencies of its coherence model.

Figure 13 (b) shows the throughput with an increasing number of nodes, each dedicating 8 worker threads per node. It illustrates CxTnL’s good scalability with the number of sharing nodes. Figure 13 (c) shows the throughput-to-median latency relationship of CxTnL and CXL-vanilla. We vary the load by increasing the number of worker threads per node from 1 to 8 while keeping 8 nodes. CxTnL is able to achieve 0.87M txn/sec with 59ms median latency in the highly contended YCSB workload, which is notably better than CXL vanilla with 0.59M txn/sec and 67ms median latency. On the less contended TPCC benchmarks, CxTnL achieves 0.92M txn/sec with stable median latency.

Figure 13 (d) shows the throughput of running all new-order transactions on CxTnL and CXL-RPCs [50, 88] as we increase the number of cross-partition transactions. To make an apple-to-apple comparison, we adopt the distributed version of DBx1000 [25] and store shared tuples at G-FAM, with each node exclusively managing 8 warehouses of TPC-C. We adopt SOTA CXL-shared memory RPC, i.e., HydraRPCs [50], which achieves 1.47us avg. latency by passing references instead of data. We test on 4 nodes, each with 8 worker threads. The CXL-RPC-based shared-nothing architecture is the optimal solution for perfectly partitionable workloads due to minimized cross-node coherence [17]. However, when roughly 20% of transactions touch multiple partitions, the throughput of the CXL-RPC architecture drops below CxTnL.

6.4 Detailed analysis of CxTnL

CXL Overhead Breakdown. Figure 15 reports the latency breakdown on G-FAM accesses with the configuration of the

SILO algorithm, no logging, and a hash index. We break down the time into DRAM accessing time, which includes the time spent on the CXL IP and DRAM controller, remote signaling time, and snoop filter querying and back invalidation time. The numbers are averaged across all loads and stores towards the G-FAM address segment, including accesses that hit local caches. CTXNL reduces the average remote signaling cost by 65.9% in the prototype and 70.8% at the ASIC. CTXNL also reduces back invalidation overheads by 87.1% and 96.5% at maximum, respectively, due to the reduced SF conflicts and queries on records. Despite the endpoint logic increasing by 34.6% and 44.4% due to CTXNL-introduced overheads, the overall cost reduces by 40.2% and 23.7%, respectively.

Primitive Distribution. Figure 14 (a) shows that 73.8% of G-FAM accesses are CTXNL primitives, while only 26.2% are CXL-vanilla for synchronization. Note that the fraction of CTXNL primitives could be larger in real-world applications due to larger record sizes and fine-grained primitive binds.

L-Ld/L-St Overheads. We further test the overheads of the CTXNL architecture. Figure 14 (b) illustrates the distribution of un-core latency for accesses that actually touch the G-FAM node. It shows that more than 50% of G-FAM accesses take less than 500ns, and 90% of accesses are bounded within 750ns. Given the zero-load CXL .mem latency is around 480ns, the overhead of the view translation flow is limited to 270ns, which is 56.2% relative to zero-load CXL .mem latency. The p99 latency reaches 1250ns since it takes the CXL-vanilla primitive and causes back-invalidation.

View Type Distribution. Figure 14 (c) shows the usage of VMS. It indicates that almost all view accesses are served by processors’ caches and less than 0.2% of views overflow to the VMS, thanks to the recent trend in processor design, which enlarges available on-chip caches by increasing L2 caches. Moreover, the VMS filter efficiently sifts out 96.1% of VAT queries that might involve additional overheads.

Coherence Traffic. Figure 14 (d) shows the usage of internal bandwidth between CTHWs. In a 16-node scenario, the cross-node view synchronization traffic only takes up 8.54 GB/s at p99 usage. The bus usage is always under 12% for a 512-bit bus working at 1GHz. This shows that the essential cross-node coherence traffic is in fact low, and our loosely coherent CTXNL primitive successfully exploits this.

6.5 Generality to Software Policies

Concurrency Control Sensitivity. To demonstrate the wide compatibility to the wide range use cases, We first investigate the impact of transaction processing policies on system performance at Figure 16 (a). CTXNL exhibits broad performance improvement with average 1.90x on all algorithms. The OCC [41] and SILO [75] gains the highest speedup by the factor of 2.26x and 2.06x due to their speculative execution that always access the entire read/write set despite of aborts. 2PL-variant policies such as NO_WAIT and WAIT_DIE [8] gain lower speedups, i.e. 30.7% and 20.3% on

average at TPC-C benchmarks, since they are bottlenecked by the lock managers at most cases [86].

Record Size Sensitivity. As Figure 16 (b) shows, CTXNL achieves higher speedup on the large record size, since it directly reduce the coherence maintenance cost on record memory accesses. This figure adopts a SILO concurrency control at the FPGA setup, with the fixed 8 byte meta-data [75]. By increasing the YCSB record size from 100B to 1KB per tuple, the speedup increases from 1.22x to 5.81x accordingly. This result demonstrates CTXNL’s opportunity for the applications with large record size.

Index Sensitivity. Figure 16 (c) shows CTXNL’s generality to hash indexes and binary tree indexes [51, 86] in TPC-C benchmarks. Despite the current index design is bounded to original CXL vanilla primitives that could not directly benefit from CTXNL primitives, we still achieve 1.72x and 1.98x performance improvement on hash and binary trees respectively, since CTXNL avoid the SF eviction traffic from tracking large records.

6.6 Scalability Tests

VAT Scalability. Figure. 17 (a) illustrates the relationship between the total pending write capacity of transactions and the number of VAT retries required for successful element insertion. We build a single-node synthesized-benchmark that generates random 64-byte L-St requests until the VAT reaches the maximum retry threshold (set as 64). The host CPU owns 32 cores and each has 3.85MB on-chip caches and adopts random eviction strategy on cache conflict. A cuckoo hash table occupies 4MB DRAM accommodating 512K entries. The results demonstrate that when the number of pending writes is relatively small (less than 20 MB), the insertion is often successful on the first attempt or requires only a few retries. As the write capacity increases, the insertion performance deteriorates. But we could keep the number of retries under 6 by maintaining the VAT occupation under 0.6. Under our default setup, the system could support the application with the write set capacity of 27MB, 52MB, and 112MB per node with the configurations using 1, 4, and 16 cuckoo hash tables, respectively.

Default VF and VBF can hold about 1.4K and 53K items at about 25% false-positive rate. Note that the default configuration of the CTHW is based on the general OLTP workloads, to optimize for applications with larger pending write sets, users could enlarge the default size or adopt pessimistic concurrency controls such as 2PL variants [86].

Link Latency. The CXL specification 2.0 introduces the CXL switches to facilitate connectivity in large-scale clusters. However, incorporating CXL switches, along with necessary retimers, significantly increases the link latency. To study the CTXNL sensitivity on link latency, we conduct a what-if analysis by adjusting C2C and C2M latency from hundreds of nanoseconds to several microseconds. Figure. 17 (b) depicts the throughput improvement of CTXNL over the CXL-vanilla

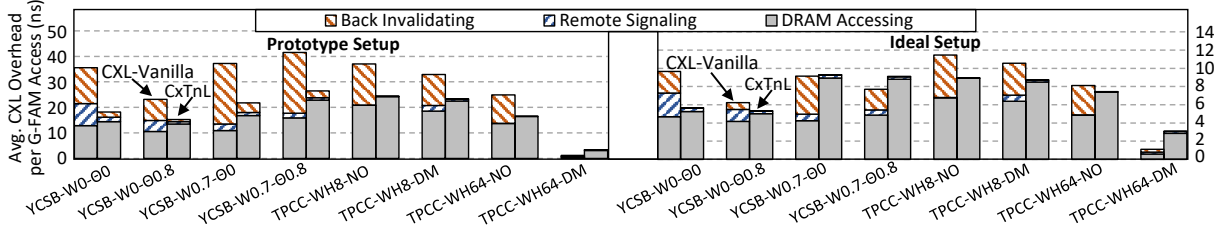


Figure 15. CXL-related overhead breakdown.

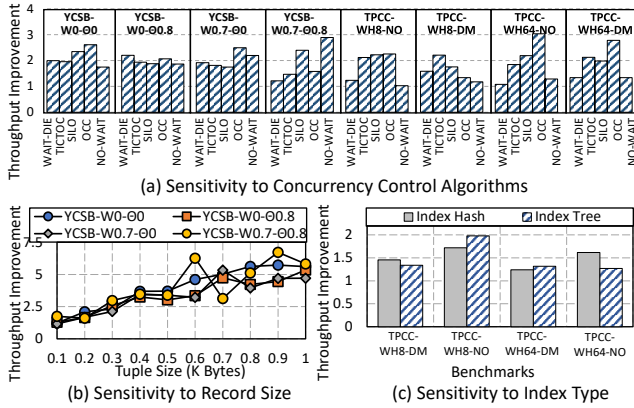


Figure 16. Generality Tests

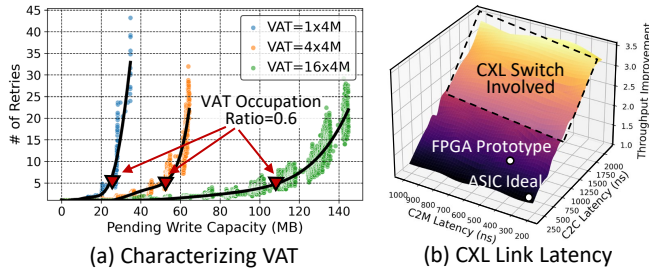


Figure 17. Scalability Tests

baseline. We test SILO algorithm on the TPC-C benchmark with 8 nodes and 8 threads each. We could tell that CXL link latency positively related to performance improvement due to its direct impact on the C2C overheads. CTXNL can achieve a throughput improvement of up to 3.41x when the CXL link takes near 1ms.

These findings indicate that the advantages of CTXNL grow as the cluster size increases. However, we suggest that the sweetpoint scale for CTXNL is when the C2C and C2M roundtrip latency is below one microsecond, which is typically a rack containing 8-16 nodes with direct connection to shared memory [43]. Because within the host processors, CXL accessing datapath share many latency hiding modules, such as store buffers and miss-status handling registers, with main memory accessing datapath. Excessive

latency in CXL memory access may overwhelm these modules and effect main memory accessing performance.

7 Discussion

7.1 Scaling issues beyond a rack

As we discussed in last section, we believe that a rack with 8-16 nodes is the sweetpoint scale for CTXNL, and beyond a rack, we anticipate the need for a heterogeneous interconnection approach, where intra-rack communication leverages CxTnL to enable efficient memory sharing, and inter-rack communication relies on traditional networks such as Ethernet or RDMA. The reasons are twofold.

Broadcasting limitations. CTXNL adopts a broadcasting-based coherence design to avoid SF bottlenecks, but this scheme does not scale well with an increasing number of nodes due to the flooding snooping traffic. Within a rack, the broadcasting field with up to 16 nodes could be efficiently supported by an in-device hardware bus, while scaling beyond a rack requires multiple CxTnL devices working in a distributed way due to I/O port limitations [43]. This introduces costly cross-device communication for broadcasting.

Node Failure Issues. Fault tolerance is crucial in large-scale transaction processing systems. To maximize the efficiency of the critical path, CTXNL hardware does not implement failure recovery mechanisms. CxTnL will stops the world and raises a hardware error when probes a node failure, and relies on the transaction processing frameworks to ensure data consistency. Consequently, the scale of CTXNL's becomes the blast radius of one node failure. By limiting CTXNL within a rack, a system can isolate blast regions using network-based fault-tolerance protocols such as 2PC.

7.2 Related works

Weak Consistency Models. A consistency model defines the contract between hardware architecture and software developers, specifying the expected behavior of a memory load. For software developers, the most intuitive model is sequential consistency [42], which maintains program order and write atomicity for parallel processes. To boost hardware performance, prior works [4, 5, 38, 89, 90] have explored a variety of weaker consistency models by relaxing certain guarantees of sequential consistency. CTXNL adopts the consistency model similar to release consistency [4, 7, 37, 59] which

preserves a partial order of memory accesses. CTXNL details how this consistency model benefits CXL-based memory sharing and provides holistic hardware and software design. **Distributed Transaction Processing.** Distributed transaction processing frameworks can be categorized into two main architectures: shared-nothing and shared-data. For decades, the shared-nothing architecture has dominated distributed database management systems, primarily due to its efficiency in minimizing network communication [11, 15, 25, 49, 73, 76]. The shared-data architecture allows transactions to access and modify data across any node within the system [34, 34, 35, 39, 45, 56, 64, 80, 81]. CTXNL design adheres to shared-data architectures but also offers potential benefits to shared-nothing architectures by optimizing conventional network communication primitives, such as HydraRPC [50].

8 Conclusion

The emergence of advanced interconnection techniques CXL enables us to rethink the distributed transactions. To overcome the performance drawbacks of CXL’s vanilla coherence model, this work proposes CTXNL, a software-hardware co-designed system that implements a novel hybrid coherence primitive tailored to the loosely coherent nature of transaction processing systems. Evaluations on OLTP benchmarks demonstrate the benefits of CTXNL, which achieves 2.08x higher throughput than CXL-vanilla primitives and exhibits unified performance improvements on various transaction processing policies.

References

- [1] S. V. Adve and M. D. Hill, “Retrospective: Weak ordering - A new definition,” in *25 Years of the International Symposia on Computer Architecture (Selected Papers)*, G. S. Sohi, Ed. ACM, 1998, pp. 63–66. [Online]. Available: <https://doi.org/10.1145/285930.285956>
- [2] M. Ahn, A. Chang, D. Lee, J. Gim, J. Kim, J. Jung, O. Rebholz, V. Pham, K. T. Malladi, and Y. Ki, “Enabling CXL memory expansion for in-memory database management systems,” in *DaMoN 2022*, S. Blanas and N. May, Eds. ACM, 2022, pp. 8:1–8:5. [Online]. Available: <https://doi.org/10.1145/3533737.3535090>
- [3] M. Alian, Y. Yuan, J. Zhang, R. Wang, M. Jung, and N. S. Kim, “Data direct I/O characterization for future I/O system exploration,” in *IEEE International Symposium on Performance Analysis of Systems and Software, ISPASS 2020, Boston, MA, USA, August 23-25, 2020*. IEEE, 2020, pp. 160–169. [Online]. Available: <https://doi.org/10.1109/ISPASS48437.2020.00031>
- [4] J. Alsop, M. S. Orr, B. M. Beckmann, and D. A. Wood, “Lazy release consistency for gpus,” in *49th Annual IEEE/ACM International Symposium on Microarchitecture, MICRO 2016, Taipei, Taiwan, October 15-19, 2016*. IEEE Computer Society, 2016, pp. 26:1–26:13. [Online]. Available: <https://doi.org/10.1109/MICRO.2016.7783729>
- [5] J. Alsop, M. D. Sinclair, and S. V. Adve, “Spandex: A flexible interface for efficient heterogeneous coherence,” in *45th ACM/IEEE Annual International Symposium on Computer Architecture, ISCA 2018, Los Angeles, CA, USA, June 1-6, 2018*, M. Annavaram, T. M. Pinkston, and B. Falsafi, Eds. IEEE Computer Society, 2018, pp. 261–274. [Online]. Available: <https://doi.org/10.1109/ISCA.2018.00031>
- [6] E. Atoofian, “Acceleration of software transactional memory through hardware clock,” in *Proceedings of the 2nd International Workshop on Many-core Embedded Systems, MES’2014, in conjunction with the 41st International Symposium on Computer Architecture, ISCA’2014, Minneapolis, MN, USA, June 15, 2014*, M. Daneshmand, M. Ebrahimi, M. Palesi, F. Angiolini, and J. Plosila, Eds. ACM, 2014, pp. 41–47. [Online]. Available: <https://doi.org/10.1145/2613908.2613912>
- [7] J. K. Bennett, J. B. Carter, and W. Zwaenepoel, “Munin: Distributed shared memory based on type-specific memory coherence,” in *Proceedings of the Second ACM SIGPLAN Symposium on Principles & Practice of Parallel Programming (PPoPP), Seattle, Washington, USA, March 14-16, 1990*, D. A. Padua, Ed. ACM, 1990, pp. 168–176. [Online]. Available: <https://doi.org/10.1145/99163.99182>
- [8] P. A. Bernstein and N. Goodman, “Concurrency control in distributed database systems,” *ACM Comput. Surv.*, vol. 13, no. 2, p. 185–221, jun 1981. [Online]. Available: <https://doi.org/10.1145/356842.356846>
- [9] Q. Cai, W. Guo, H. Zhang, D. Agrawal, G. Chen, B. C. Ooi, K. Tan, Y. M. Teo, and S. Wang, “Efficient distributed memory management with RDMA and caching,” *Proc. VLDB Endow.*, vol. 11, no. 11, pp. 1604–1617, 2018. [Online]. Available: <http://www.vldb.org/pvldb/vol11/p1604-cai.pdf>
- [10] T. E. Carlson, W. Heirman, and L. Eeckhout, “Sniper: Exploring the level of abstraction for scalable and accurate parallel multi-core simulation,” in *SC 11*, S. A. Lathrop, J. Costa, and W. Kramer, Eds., 2011. [Online]. Available: <https://doi.org/10.1145/2063384.2063454>
- [11] J. Chen, S. Jindel, R. Walzer, R. Sen, N. Jimsheleishvili, and M. Andrews, “The memsql query optimizer: A modern optimizer for real-time analytics in a distributed database,” *Proc. VLDB Endow.*, vol. 9, no. 13, pp. 1401–1412, 2016. [Online]. Available: <http://www.vldb.org/pvldb/vol9/p1401-chen.pdf>
- [12] B. Choi, R. Komuravelli, H. Sung, R. Smolinski, N. Honarmand, S. V. Adve, V. S. Adve, N. P. Carter, and C. Chou, “Denovo: Rethinking the memory hierarchy for disciplined parallelism,” in *2011 International Conference on Parallel Architectures and Compilation Techniques, PACT 2011, Galveston, TX, USA, October 10-14, 2011*, L. Rauchwerger and V. Sarkar, Eds. IEEE Computer Society, 2011, pp. 155–166. [Online]. Available: <https://doi.org/10.1109/PACT.2011.21>
- [13] B. F. Cooper, A. Silberstein, E. Tam, R. Ramakrishnan, and R. Sears, “Benchmarking cloud serving systems with ycsb,” in *SoCC ’10*, J. M. Hellerstein, S. Chaudhuri, and M. Rosenblum, Eds., 2010, p. 143–154. [Online]. Available: <https://doi.org/10.1145/1807128.1807152>
- [14] I. Corporation, “Intel® fpga compute express link (cxl) ip,” <https://www.intel.com/content/www/us/en/products/details/fpga/intellectual-property/interface-protocols/cxl-ip.html>, 2024.
- [15] U. Cubukcu, O. Erdogan, S. Pathak, S. Sannakkayala, and M. Slot, “Citrus: Distributed postgresql for data-intensive applications,” in *SIGMOD ’21: International Conference on Management of Data, Virtual Event, China, June 20-25, 2021*, G. Li, Z. Li, S. Idreos, and D. Srivastava, Eds. ACM, 2021, pp. 2490–2502. [Online]. Available: <https://doi.org/10.1145/3448016.3457551>
- [16] CXL Consortium, “Compute express link specification revision 3.0.” [Online]. Available: <https://www.computeexpresslink.org/download-the-specification>
- [17] C. Diaconu, C. Freedman, E. Ismert, P. Larson, P. Mittal, R. Stonecipher, N. Verma, and M. Zwilling, “Hekaton: SQL server’s memory-optimized OLTP engine,” in *Proceedings of the ACM SIGMOD International Conference on Management of Data, SIGMOD 2013, New York, NY, USA, June 22-27, 2013*, K. A. Ross, D. Srivastava, and D. Papadias, Eds. ACM, 2013, pp. 1243–1254. [Online]. Available: <https://doi.org/10.1145/2463676.2463710>
- [18] A. Dragojevic, D. Narayanan, M. Castro, and O. Hodson, “Farm: Fast remote memory,” in *Proceedings of the 11th USENIX Symposium on Networked Systems Design and Implementation, NSDI 2014, Seattle, WA, USA, April 2-4, 2014*, R. Mahajan and I. Stoica, Eds. USENIX Association, 2014, pp. 401–414. [Online]. Available: <https://www.usenix.org/conference/nsdi14/technical-sessions/dragojevi%C4%87>

- [19] A. Dragojevic, D. Narayanan, E. B. Nightingale, M. Renzelmann, A. Shamis, A. Badam, and M. Castro, “No compromises: distributed transactions with consistency, availability, and performance,” in *SOSP 2015, Monterey, CA, USA, October 4-7, 2015*, E. L. Miller and S. Hand, Eds. ACM, 2015, pp. 54–70. [Online]. Available: <https://doi.org/10.1145/2815400.2815425>
- [20] D. Duplyakin, R. Ricci, A. Maricq, G. Wong, J. Duerig, E. Eide, L. Stoller, M. Hibler, D. Johnson, K. Webb, A. Akella, K. Wang, G. Ricart, L. Landweber, C. Elliott, M. Zink, E. Cecchet, S. Kar, and P. Mishra, “The design and operation of CloudLab,” in *Proceedings of the USENIX Annual Technical Conference (ATC)*, Jul. 2019, pp. 1–14. [Online]. Available: <https://www.flux.utah.edu/paper/duplyakin-atc19>
- [21] D. Fujiki, “MVC: enabling fully coherent multi-data-views through the memory hierarchy with processing in memory,” in *Proceedings of the 56th Annual IEEE/ACM International Symposium on Microarchitecture, MICRO 2023, Toronto, ON, Canada, 28 October 2023 - 1 November 2023*. ACM, 2023, pp. 800–814. [Online]. Available: <https://doi.org/10.1145/3613424.3623784>
- [22] D. Gouk, S. Lee, M. Kwon, and M. Jung, “Direct access, high-performance memory disaggregation with directcxl,” in *USENIX ATC 2022*, J. Schindler and N. Zilberman, Eds., 2022. [Online]. Available: <https://www.usenix.org/conference/atc22/presentation/gouk>
- [23] Z. Guo, Y. Shan, X. Luo, Y. Huang, and Y. Zhang, “Clío: a hardware-software co-designed disaggregated memory system,” in *ASPLOS ’22: 27th ACM International Conference on Architectural Support for Programming Languages and Operating Systems, Lausanne, Switzerland, 28 February 2022 - 4 March 2022*, B. Falsafi, M. Ferdman, S. Lu, and T. F. Wenisch, Eds. ACM, 2022, pp. 417–433. [Online]. Available: <https://doi.org/10.1145/3503222.3507762>
- [24] L. Hammond, V. Wong, M. K. Chen, B. D. Carlstrom, J. D. Davis, B. Hertzberg, M. K. Prabhu, H. Wijaya, C. Kozyrakis, and K. Olukotun, “Transactional memory coherence and consistency,” in *31st International Symposium on Computer Architecture (ISCA 2004)*, 19–23 June 2004, Munich, Germany. IEEE Computer Society, 2004, pp. 102–113. [Online]. Available: <https://doi.org/10.1109/ISCA.2004.1310767>
- [25] R. Harding, D. V. Aken, A. Pavlo, and M. Stonebraker, “An evaluation of distributed concurrency control,” *Proc. VLDB Endow.*, vol. 10, no. 5, pp. 553–564, 2017. [Online]. Available: <http://www.vldb.org/pvldb/vol10/p553-harding.pdf>
- [26] J. Helt, M. Burke, A. Levy, and W. Lloyd, “Regular sequential serializability and regular sequential consistency,” in *SOSP ’21: ACM SIGOPS 28th Symposium on Operating Systems Principles, Virtual Event / Koblenz, Germany, October 26-29, 2021*, R. van Renesse and N. Zeldovich, Eds. ACM, 2021, pp. 163–179. [Online]. Available: <https://doi.org/10.1145/3477132.3483566>
- [27] J. L. Hennessy and D. A. Patterson, *Computer Architecture - A Quantitative Approach, 5th Edition*. Morgan Kaufmann, 2012.
- [28] Intel, “Cxl protocol hard ip functionality accelerates a wide range of data-centric workloads.” [Online]. Available: <https://www.intel.com/content/www/us/en/products/details/fpga/intellectual-property/interface-protocols/cxl-ip.html#tab-blade-1-0>
- [29] Intel, “Directory structure in skylake server cpus.” [Online]. Available: <https://community.intel.com/t5/Software-Tuning-Performance/Directory-Structure-in-Skylake-Server-CPUs/m-p/1185376>
- [30] Intel, “Intel® data direct i/o technology.” [Online]. Available: <https://www.intel.com/content/www/us/en/io/data-direct-i-o-technology.html>
- [31] Intel, “Intel® memory latency checker v3.11b.” [Online]. Available: <https://www.intel.com/content/www/us/en/developer/articles/tool/intelr-memory-latency-checker.html>
- [32] —, “An introduction to the intel quickpath interconnect.” [Online]. Available: <https://www.intel.com/content/www/us/en/io/quickpath-technology/quick-path-interconnect-introduction-paper.html>
- [33] J. Jang, H. Choi, H. Bae, S. Lee, M. Kwon, and M. Jung, “CXL-ANNS: software-hardware collaborative memory disaggregation and computation for billion-scale approximate nearest neighbor search,” in *2023 USENIX Annual Technical Conference, USENIX ATC 2023, Boston, MA, USA, July 10-12, 2023*, J. Lawall and D. Williams, Eds. USENIX Association, 2023, pp. 585–600. [Online]. Available: <https://www.usenix.org/conference/atc23/presentation/jang>
- [34] E. Jeong, S. Woo, M. A. Jamshed, H. Jeong, S. Ihm, D. Han, and K. Park, “mtcp: a highly scalable user-level TCP stack for multicore systems,” in *Proceedings of the 11th USENIX Symposium on Networked Systems Design and Implementation, NSDI 2014, Seattle, WA, USA, April 2-4, 2014*, R. Mahajan and I. Stoica, Eds. USENIX Association, 2014, pp. 489–502. [Online]. Available: <https://www.usenix.org/conference/nsdi14/technical-sessions/presentation/jeong>
- [35] A. Kalia and D. G. Andersen, “Fasst: Fast, scalable and simple distributed transactions with two-sided (RDMA) datagram rpcs,” in *12th USENIX Symposium on Operating Systems Design and Implementation, OSDI 2016, Savannah, GA, USA, November 2-4, 2016*, K. Keeton and T. Roscoe, Eds. USENIX Association, 2016, pp. 185–201. [Online]. Available: <https://www.usenix.org/conference/osdi16/technical-sessions/presentation/kalia>
- [36] A. Kalia, M. Kaminsky, and D. G. Andersen, “Design guidelines for high performance RDMA systems,” in *2016 USENIX Annual Technical Conference, USENIX ATC 2016, Denver, CO, USA, June 22-24, 2016*, A. Gulati and H. Weatherspoon, Eds. USENIX Association, 2016, pp. 437–450. [Online]. Available: <https://www.usenix.org/conference/atc16/technical-sessions/presentation/kalia>
- [37] P. Keleher, A. L. Cox, S. Dwarkadas, and W. Zwaenepoel, “Tread marks: Distributed shared memory on standard workstations and operating systems,” in *USENIX Winter 1994 Technical Conference (USENIX Winter 1994 Technical Conference)*. San Francisco, CA: USENIX Association, Jan. 1994. [Online]. Available: <https://www.usenix.org/conference/usenix-winter-1994-technical-conference/tread-marks-distributed-shared-memory-standard>
- [38] P. J. Keleher, A. L. Cox, and W. Zwaenepoel, “Lazy release consistency for software distributed shared memory,” in *Proceedings of the 19th Annual International Symposium on Computer Architecture. Gold Coast, Australia, May 1992*, A. Gottlieb, Ed. ACM, 1992, pp. 13–21. [Online]. Available: <https://doi.org/10.1145/139669.139676>
- [39] J. Kim, I. Jang, W. Reda, J. Im, M. Canini, D. Kotic, Y. Kwon, S. Peter, and E. Witchel, “Línefs: Efficient smartnic offload of a distributed file system with pipeline parallelism,” in *SOSP ’21: ACM SIGOPS 28th Symposium on Operating Systems Principles, Virtual Event / Koblenz, Germany, October 26-29, 2021*, R. van Renesse and N. Zeldovich, Eds. ACM, 2021, pp. 756–771. [Online]. Available: <https://doi.org/10.1145/3477132.3483565>
- [40] K. Kim, H. Kim, J. So, W. Lee, J. Im, S. Park, J. Cho, and H. Song, “SMT: software-defined memory tiering for heterogeneous computing systems with CXL memory expander,” *IEEE Micro*, vol. 43, no. 2, pp. 20–29, 2023. [Online]. Available: <https://doi.org/10.1109/MM.2023.3240774>
- [41] H. T. Kung and J. T. Robinson, “On optimistic methods for concurrency control,” *ACM Trans. Database Syst.*, vol. 6, no. 2, p. 213–226, jun 1981. [Online]. Available: <https://doi.org/10.1145/319566.319567>
- [42] L. Lamport, “How to make a multiprocessor computer that correctly executes multiprocess programs,” *IEEE Trans. Computers*, vol. 28, no. 9, pp. 690–691, 1979. [Online]. Available: <https://doi.org/10.1109/TC.1979.1675439>
- [43] H. Li, D. S. Berger, L. Hsu, D. Ernst, P. Zardoshti, S. Novakovic, M. Shah, S. Rajadnya, S. Lee, I. Agarwal, M. D. Hill, M. Fontoura, and R. Bianchini, “Pond: Cxl-based memory pooling systems for cloud platforms,” 2022. [Online]. Available: <https://arxiv.org/abs/2203.00241>
- [44] H. Litz, D. R. Cheriton, A. Firoozshahian, O. Azizi, and J. P. Stevenson, “SI-TM: reducing transactional memory abort rates through snapshot isolation,” in *Architectural Support for Programming*

- Languages and Operating Systems, ASPLOS 2014, Salt Lake City, UT, USA, March 1-5, 2014*, R. Balasubramonian, A. Davis, and S. V. Adve, Eds. ACM, 2014, pp. 383–398. [Online]. Available: <https://doi.org/10.1145/2541940.2541952>
- [45] M. Liu, T. Cui, H. Schuh, A. Krishnamurthy, S. Peter, and K. Gupta, “Offloading distributed applications onto smartnics using ipipe,” in *Proceedings of the ACM Special Interest Group on Data Communication, SIGCOMM 2019, Beijing, China, August 19-23, 2019*, J. Wu and W. Hall, Eds. ACM, 2019, pp. 318–333. [Online]. Available: <https://doi.org/10.1145/3341302.3342079>
- [46] K. Loughlin, S. Saroiu, A. Wolman, Y. A. Manerkar, and B. Kasikci, “Moesei-prime: preventing coherence-induced hammering in commodity workloads,” in *ISCA ’22: The 49th Annual International Symposium on Computer Architecture, New York, New York, USA, June 18 - 22, 2022*, V. Salapura, M. Zahran, F. Chong, and L. Tang, Eds. ACM, 2022, pp. 670–684. [Online]. Available: <https://doi.org/10.1145/3470496.3527427>
- [47] H. Lu, C. Hodsdon, K. Ngo, S. Mu, and W. Lloyd, “The SNOW theorem and latency-optimal read-only transactions,” in *12th USENIX Symposium on Operating Systems Design and Implementation, OSDI 2016, Savannah, GA, USA, November 2-4, 2016*, K. Keeton and T. Roscoe, Eds. USENIX Association, 2016, pp. 135–150. [Online]. Available: <https://www.usenix.org/conference/osdi16/technical-sessions/presentation/lu>
- [48] H. Lu, S. Sen, and W. Lloyd, “Performance-optimal read-only transactions,” in *14th USENIX Symposium on Operating Systems Design and Implementation, OSDI 2020, Virtual Event, November 4-6, 2020*. USENIX Association, 2020, pp. 333–349. [Online]. Available: <https://www.usenix.org/conference/osdi20/presentation/lu>
- [49] L. Ma, J. Arulraj, S. Zhao, A. Pavlo, S. R. Dulloor, M. J. Giardino, J. Parkhurst, J. L. Gardner, K. A. Doshi, and S. B. Zdonik, “Larger-than-memory data management on modern storage hardware for in-memory OLTP database systems,” in *Proceedings of the 12th International Workshop on Data Management on New Hardware, DaMoN 2016, San Francisco, CA, USA, June 27, 2016*. ACM, 2016, pp. 9:1–9:7. [Online]. Available: <https://doi.org/10.1145/2933349.2933358>
- [50] T. Ma, Z. Liu, C. Wei, J. Huang, Y. Zhuo, H. Li, N. Zhang, Y. Guan, D. Niu, M. Zhang, and T. Ma, “Hydrarpc: Rpc in the cxl era,” in *2024 USENIX Annual Technical Conference, USENIX ATC 2019*. USENIX Association, 2024. [Online]. Available: <https://www.usenix.org/conference/atc24/presentation/ma>
- [51] Y. Mao, E. Kohler, and R. T. Morris, “Cache craftiness for fast multicore key-value storage,” in *European Conference on Computer Systems, Proceedings of the Seventh EuroSys Conference 2012, EuroSys ’12, Bern, Switzerland, April 10-13, 2012*, P. Felber, F. Bellosa, and H. Bos, Eds. ACM, 2012, pp. 183–196. [Online]. Available: <https://doi.org/10.1145/2168836.2168855>
- [52] L. Maranget, S. Sarkar, and P. Sewell. (2012) A tutorial introduction to the arm and power relaxed memory models. [Online]. Available: <https://www.cl.cam.ac.uk/~pes20/ppc-supplemental/test7.pdf>
- [53] H. A. Maruf, H. Wang, A. Dhanotia, J. Weiner, N. Agarwal, P. Bhattacharya, C. Petersen, M. Chowdhury, S. O. Kanaujia, and P. Chauhan, “TPP: transparent page placement for cxl-enabled tiered-memory,” in *Proceedings of the 28th ACM International Conference on Architectural Support for Programming Languages and Operating Systems, Volume 3, ASPLOS 2023, Vancouver, BC, Canada, March 25-29, 2023*, T. M. Aamodt, N. D. E. Jerger, and M. M. Swift, Eds. ACM, 2023, pp. 742–755. [Online]. Available: <https://doi.org/10.1145/3582016.3582063>
- [54] K. E. Moore, J. Bobba, M. J. Moravan, M. D. Hill, and D. A. Wood, “Logtm: log-based transactional memory,” in *12th International Symposium on High-Performance Computer Architecture, HPCA-12 2006, Austin, Texas, USA, February 11-15, 2006*. IEEE Computer Society, 2006, pp. 254–265. [Online]. Available: <https://doi.org/10.1109/HPCA.2006.1598134>
- [55] V. Nagarajan, D. J. Sorin, M. D. Hill, D. A. Wood, and N. E. Jerger, *A Primer on Memory Consistency and Cache Coherence*, 2nd ed. Morgan & Claypool Publishers, 2020.
- [56] J. Nelson, B. Holt, B. Myers, P. Briggs, L. Ceze, S. Kahan, and M. Oskin, “Latency-tolerant software distributed shared memory,” in *2015 USENIX Annual Technical Conference, USENIX ATC ’15, July 8-10, Santa Clara, CA, USA*, S. Lu and E. Riedel, Eds. USENIX Association, 2015, pp. 291–305. [Online]. Available: <https://www.usenix.org/conference/atc15/technical-session/presentation/nelson>
- [57] R. Pagh and F. F. Rodler, “Cuckoo hashing,” in *Algorithms - ESA 2001, 9th Annual European Symposium, Aarhus, Denmark, August 28-31, 2001, Proceedings*, ser. Lecture Notes in Computer Science, F. M. auf der Heide, Ed., vol. 2161. Springer, 2001, pp. 121–133. [Online]. Available: https://doi.org/10.1007/3-540-44676-1_10
- [58] PMem.io, “Persistent Memory Development Kit (PMDK),” <https://pmem.io/pmdk/>.
- [59] D. R. K. Ports, A. T. Clements, I. Zhang, S. Madden, and B. Liskov, “Transactional consistency and automatic management in an application data cache,” in *9th USENIX Symposium on Operating Systems Design and Implementation, OSDI 2010, October 4-6, 2010, Vancouver, BC, Canada, Proceedings*, R. H. Arpaci-Dusseau and B. Chen, Eds. USENIX Association, 2010, pp. 279–292. [Online]. Available: http://www.usenix.org/events/osdi10/tech/full_papers/Ports.pdf
- [60] D. Qin, A. D. Brown, and A. Goel, “Caracal: Contention management with deterministic concurrency control,” in *SOSP ’21: ACM SIGOPS 28th Symposium on Operating Systems Principles, Virtual Event / Koblenz, Germany, October 26-29, 2021*, R. van Renesse and N. Zeldovich, Eds. ACM, 2021, pp. 180–194. [Online]. Available: <https://doi.org/10.1145/3477132.3483591>
- [61] R. Rajwar, M. Herlihy, and K. K. Lai, “Virtualizing transactional memory,” in *32nd International Symposium on Computer Architecture (ISCA 2005), 4-8 June 2005, Madison, Wisconsin, USA*. IEEE Computer Society, 2005, pp. 494–505. [Online]. Available: <https://doi.org/10.1109/ISCA.2005.54>
- [62] S. Sarkar, P. Sewell, J. Alglave, L. Maranget, and D. Williams, “Understanding POWER multiprocessors,” in *Proceedings of the 32nd ACM SIGPLAN Conference on Programming Language Design and Implementation, PLDI 2011, San Jose, CA, USA, June 4-8, 2011*, M. W. Hall and D. A. Padua, Eds. ACM, 2011, pp. 175–186. [Online]. Available: <https://doi.org/10.1145/1993498.1993520>
- [63] H. N. Schuh, A. Krishnamurthy, D. Culler, H. M. Levy, L. Rizzo, S. Khan, and B. E. Stephens, “Cc-nic: a cache-coherent interface to the nic,” in *Proceedings of the 29th ACM International Conference on Architectural Support for Programming Languages and Operating Systems, Volume 1*, ser. ASPLOS ’24. New York, NY, USA: Association for Computing Machinery, 2024, p. 52–68. [Online]. Available: <https://doi.org/10.1145/3617232.3624868>
- [64] H. N. Schuh, W. Liang, M. Liu, J. Nelson, and A. Krishnamurthy, “Xenic: Smartnic-accelerated distributed transactions,” in *SOSP ’21: ACM SIGOPS 28th Symposium on Operating Systems Principles, Virtual Event / Koblenz, Germany, October 26-29, 2021*, R. van Renesse and N. Zeldovich, Eds. ACM, 2021, pp. 740–755. [Online]. Available: <https://doi.org/10.1145/3477132.3483555>
- [65] V. Seshadri, G. Pekhimenko, O. Ruwase, O. Mutlu, P. B. Gibbons, M. A. Kozuch, T. C. Mowry, and T. M. Chilimbi, “Page overlays: an enhanced virtual memory framework to enable fine-grained memory management,” in *Proceedings of the 42nd Annual International Symposium on Computer Architecture, Portland, OR, USA, June 13-17, 2015*, 2015, pp. 79–91. [Online]. Available: <https://doi.org/10.1145/2749469.2750379>
- [66] Y. Shan, Y. Huang, Y. Chen, and Y. Zhang, “Legoos: A disseminated, distributed OS for hardware resource disaggregation,” in *2019 USENIX Annual Technical Conference, USENIX ATC 2019, Renton, WA, USA, July 10-12, 2019*, D. Malkhi and D. Tsafir, Eds. USENIX Association,

2019. [Online]. Available: <https://www.usenix.org/conference/atc19/presentation/shan>
- [67] D. D. Sharma, "Compute express link®: An open industry-standard interconnect enabling heterogeneous data-centric computing," in *HOTI 2022*. IEEE, 2022, pp. 5–12. [Online]. Available: <https://doi.org/10.1109/HOTI55740.2022.00017>
- [68] D. D. Sharma, R. Blankenship, and D. S. Berger, "An introduction to the compute express link (cxl) interconnect," 2024.
- [69] A. Shriraman, S. Dwarkadas, and M. L. Scott, "Flexible decoupled transactional memory support," in *35th International Symposium on Computer Architecture (ISCA 2008)*, June 21-25, 2008, Beijing, China. IEEE Computer Society, 2008, pp. 139–150. [Online]. Available: <https://doi.org/10.1109/ISCA.2008.17>
- [70] A. Shriraman, M. F. Spear, H. Hossain, V. J. Marathe, S. Dwarkadas, and M. L. Scott, "An integrated hardware-software approach to flexible transactional memory," in *34th International Symposium on Computer Architecture (ISCA 2007)*, June 9-13, 2007, San Diego, California, USA, D. M. Tullsen and B. Calder, Eds. ACM, 2007, pp. 104–115. [Online]. Available: <https://doi.org/10.1145/1250662.1250676>
- [71] D. Skarlatos, A. Kokolis, T. Xu, and J. Torrellas, "Elastic cuckoo page tables: Rethinking virtual memory translation for parallelism," in *ASPLOS '20: Architectural Support for Programming Languages and Operating Systems, Lausanne, Switzerland, March 16-20, 2020*, J. R. Larus, L. Ceze, and K. Strauss, Eds. ACM, 2020, pp. 1093–1108. [Online]. Available: <https://doi.org/10.1145/3373376.3378493>
- [72] Y. Sun, Y. Yuan, Z. Yu, R. Kuper, I. Jeong, R. Wang, and N. S. Kim, "Demystifying CXL memory with genuine cxl-ready systems and devices," *CoRR*, vol. abs/2303.15375, 2023. [Online]. Available: <https://doi.org/10.48550/arXiv.2303.15375>
- [73] A. Thomson, "Calvin: fast distributed transactions for partitioned database systems," in *Proceedings of the ACM SIGMOD International Conference on Management of Data, SIGMOD 2012, Scottsdale, AZ, USA, May 20-24, 2012*. ACM, 2012, pp. 1–12. [Online]. Available: <https://doi.org/10.1145/2213836.2213838>
- [74] TPC-C, "Tpc benchmark c. <https://www.tpc.org/tpcc/>" [Online]. Available: <https://www.tpc.org/tpcc/>
- [75] S. Tu, W. Zheng, E. Kohler, B. Liskov, and S. Madden, "Speedy transactions in multicore in-memory databases," in *SOSP*, M. Kaminsky and M. Dahlin, Eds. New York, NY, USA: Association for Computing Machinery, 2013, p. 18–32. [Online]. Available: <https://doi.org/10.1145/2517349.2522713>
- [76] VoltDB, "Voltdb." [Online]. Available: <https://www.voltdb.com/>
- [77] J. Wang, D. Ding, H. Wang, C. Christensen, Z. Wang, H. Chen, and J. Li, "Polyjuice: High-Performance transactions via learned concurrency control," in *15th USENIX Symposium on Operating Systems Design and Implementation (OSDI 21)*. USENIX Association, Jul. 2021, pp. 198–216. [Online]. Available: <https://www.usenix.org/conference/osdi21/presentation/wang-jiachen>
- [78] Z. Wang, M. A. Kozuch, T. C. Mowry, and V. Seshadri, "Multiversed page overlays: Enabling faster serializable hardware transactional memory," in *28th International Conference on Parallel Architectures and Compilation Techniques, PACT 2019, Seattle, WA, USA, September 23-26, 2019*. IEEE, 2019, pp. 395–408. [Online]. Available: <https://doi.org/10.1109/PACT.2019.00038>
- [79] X. Wei, R. Chen, H. Chen, and B. Zang, "Xstore: Fast rdma-based ordered key-value store using remote learned cache," *ACM Trans. Storage*, vol. 17, no. 3, pp. 18:1–18:32, 2021. [Online]. Available: <https://doi.org/10.1145/3468520>
- [80] X. Wei, Z. Dong, R. Chen, and H. Chen, "Deconstructing rdma-enabled distributed transactions: Hybrid is better!" in *13th USENIX Symposium on Operating Systems Design and Implementation, OSDI 2018, Carlsbad, CA, USA, October 8-10, 2018*, A. C. Arpaci-Dusseau and G. Voelker, Eds. USENIX Association, 2018, pp. 233–251. [Online]. Available: <https://www.usenix.org/conference/osdi18/presentation/wei>
- [81] X. Wei, J. Shi, Y. Chen, R. Chen, and H. Chen, "Fast in-memory transaction processing using RDMA and HTM," in *SOSP 2015, Monterey, CA, USA, October 4-7, 2015*, E. L. Miller and S. Hand, Eds. ACM, 2015, pp. 87–104. [Online]. Available: <https://doi.org/10.1145/2815400.2815419>
- [82] Y. Wu, J. He, S. Yan, J. Wu, T. Yang, O. Ruas, G. Zhang, and B. Cui, "Elastic bloom filter: Deletable and expandable filter using elastic fingerprints," *IEEE Trans. Computers*, vol. 71, no. 4, pp. 984–991, 2022. [Online]. Available: <https://doi.org/10.1109/TC.2021.3067713>
- [83] Y. Xia, X. Yu, A. Pavlo, and S. Devadas, "Taurus: Lightweight parallel logging for in-memory database management systems," *Proc. VLDB Endow.*, vol. 14, no. 2, pp. 189–201, 2020. [Online]. Available: <http://www.vldb.org/pvldb/vol14/p189-xia.pdf>
- [84] Xilinx, "Hash crypto engine. <https://www.xilinx.com/products/intellectual-property/1-48zyr.html>." [Online]. Available: <https://www.xilinx.com/products/intellectual-property/1-48zyr.html>
- [85] M. Yan, R. Sprabery, B. Gopireddy, C. W. Fletcher, R. H. Campbell, and J. Torrellas, "Attack directories, not caches: Side channel attacks in a non-inclusive world," in *2019 IEEE Symposium on Security and Privacy, SP 2019, San Francisco, CA, USA, May 19-23, 2019*. IEEE, 2019, pp. 888–904. [Online]. Available: <https://doi.org/10.1109/SP.2019.00004>
- [86] X. Yu, G. Bezerra, A. Pavlo, S. Devadas, and M. Stonebraker, "Staring into the abyss: An evaluation of concurrency control with one thousand cores," *Proc. VLDB Endow.*, vol. 8, no. 3, pp. 209–220, 2014. [Online]. Available: <http://www.vldb.org/pvldb/vol8/p209-yu.pdf>
- [87] E. Zamanian, C. Binnig, T. Kraska, and T. Harris, "The end of a myth: Distributed transactions can scale," *Proc. VLDB Endow.*, vol. 10, no. 6, p. 685–696, feb 2017. [Online]. Available: <https://doi.org/10.14778/3055330.3055335>
- [88] M. Zhang, T. Ma, J. Hua, Z. Liu, K. Chen, N. Ding, F. Du, J. Jiang, T. Ma, and Y. Wu, "Partial failure resilient memory management system for (cxl-based) distributed shared memory," in *Proceedings of the 29th Symposium on Operating Systems Principles, SOSP 2023, Koblenz, Germany, October 23-26, 2023*, J. Flinn, M. I. Seltzer, P. Druschel, A. Kaufmann, and J. Mace, Eds. ACM, 2023, pp. 658–674. [Online]. Available: <https://doi.org/10.1145/3600006.3613135>
- [89] S. Zhang, M. Vijayaraghavan, and Arvind, "Weak memory models: Balancing definitional simplicity and implementation flexibility," in *26th International Conference on Parallel Architectures and Compilation Techniques, PACT 2017, Portland, OR, USA, September 9-13, 2017*. IEEE Computer Society, 2017, pp. 288–302. [Online]. Available: <https://doi.org/10.1109/PACT.2017.29>
- [90] S. Zhang, M. Vijayaraghavan, A. Wright, M. Alipour, and Arvind, "Constructing a weak memory model," in *45th ACM/IEEE Annual International Symposium on Computer Architecture, ISCA 2018, Los Angeles, CA, USA, June 1-6, 2018*, M. Annavaram, T. M. Pinkston, and B. Falsafi, Eds. IEEE Computer Society, 2018, pp. 124–137. [Online]. Available: <https://doi.org/10.1109/ISCA.2018.00021>
- [91] Z. Zhou, Y. Chen, T. Zhang, Y. Wang, R. Shu, S. Xu, P. Cheng, L. Qu, Y. Xiong, and G. Sun, "Toward cxl-native memory tiering via device-side profiling," 2024.